

# Experimental and Numerical Analysis of the Friction Welding Process for the 4340 Steel and Mild Steel Combinations

*A model was developed that can be used as an industrial tool to predict evolution of temperature, stress, strain, and final geometry of the welded parts*

BY S. A. A. AKBARI MOUSAVI AND A. RAHBAR KELISHAMI

**ABSTRACT.** During friction welding, temperature, stress, strain, and their variations govern welding parameters, and knowledge of them helps determine optimum parameters and ways to improve the design and manufacture of welding machines. The finite element method was used for the coupled thermomechanical problem, and the Johnson-Cook equation was used to define material properties. The variations in temperature, deformation, stress, strain, and strain rate during continuous welding were systematically investigated and analyzed. The calculated results of temperature distribution were in good agreement with the infrared detected ones. The numerically calculated results for the shape of the welded joint also showed an excellent fit with the experimental observations. The effects of initial and final pressure on internal parameters are discussed. Moreover, the metallographical examinations, hardness, and tensile tests of the samples were carried out. In addition, in this study, the operational parameters of the friction welding process are related to the physical parameters of the process.

## Introduction

Friction welding is a complicated metallurgical process, accompanied by a series of physical phenomena: frictional heat generation, plastic deformation, cooling of high-temperature metal, and solid-state phase variation. In the continuous-drive friction welding processes, the thermomechanical behavior at the interface is obviously critical to the quality of the welded joint. Friction welding is a process in which the heat for welding is produced by direct conversion of mechan-

ical energy to thermal energy at the interface of the workpieces. In order to model the friction welding process, a combination of thermal effects and plastic deformation is needed.

The friction welding process is a solid-state joining process that produces a weld under the compressive force contact of one rotating and one stationary workpiece. The heat is generated at the weld interface because of the continuous rubbing of contact surfaces, which, in turn, causes a temperature rise and subsequent softening of material. Eventually, the material at the interface starts to flow plastically and forms an upset. When a certain amount of upsetting has occurred, the rotation stops and the compressive force is maintained or slightly increased to consolidate the weld. Friction time, friction pressure, forging time, upset time, forging pressure, and rotation speed are the most important operational parameters in the friction welding process.

Few attempts have been carried out in the literature to simulate the friction welding process. In these studies, only one or two of the operational parameters were discussed. Most of the simulations were performed for the stir and inertia friction welding processes. Only a few efforts were reported in the literature for the continuous friction welding process. Vairis et al. (Ref. 1) simulated linear friction welding of titanium bars. He predicted the temperature rise in the initial phase of the process. Sluzalec (Ref. 2) used the finite element method (FEM) to determine the

stress and strain distributions during the welding process. Fu et al. (Ref. 3) simulated deformation and transient temperature during the process by the finite element method. Alvise et al. (Ref. 4) simulated the two-dimensional inertia friction welding process for two dissimilar materials, though the names of the materials modeled were not reported. Recently, Sahin (Ref. 5) introduced a friction subroutine in his visual basic program to model the shape of the upset in the continuous friction welding process.

In this study, friction welding experiments were carried out for 4340 and mild steel combinations. The various materials were used to validate the simulation results. All of the experiments performed were modeled using the ABAQUS code and under similar conditions. The physical parameters such as temperature, stress, strain, and strain rate fields for a friction welded joint of a few materials in bar form were calculated under given boundary conditions. Variable thermal and mechanical properties of the welded material were taken into account. The simulation results were validated against the experiments. An infrared detector was used to measure the temperature at the contact surface of the weldment. The infrared detector results are compared with the simulated values. The observed shape of the welded joint is also compared with the simulated one. In all the tension tests carried out, the samples were broken from their base metals and not the welds. The metallographical examinations of the specimens were also performed. Moreover, in this study, the operational parameters of the friction welding process are related to the physical parameters of the process.

## Experimental Samples

Experiments were carried out to friction weld the samples with 20-mm diame-

### KEYWORDS

Friction Welding  
Finite Element Method  
Mechanical Properties

*S. A. A. AKBAR MOUSAVI and A. RAHBAR KELISHAMI are with the School of Metallurgy and Materials Engineering, University College of Engineering, University of Tehran, Tehran, Iran. E-mail Mousavi at mousavi@engmail.ut.ac.ir.*

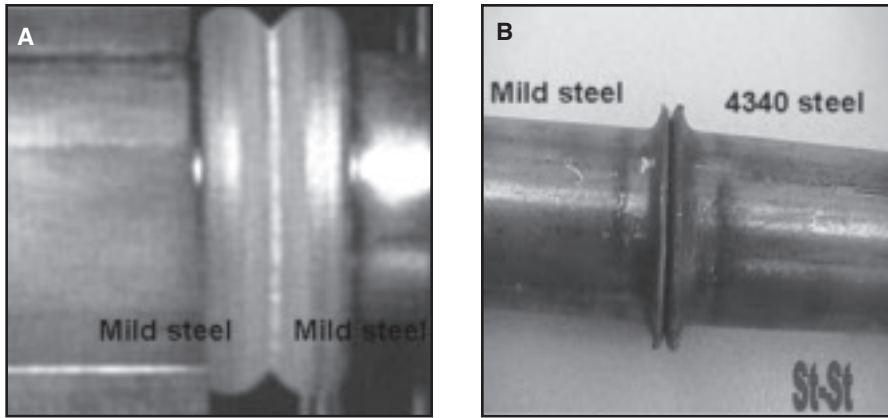


Fig. 1 — The final shape of the following friction welds: A — Mild steel to mild steel; B — 4340 steel to mild steel.

ters and 100-mm lengths. The operational parameters of the process for the similar and dissimilar materials welded are tabulated in Table 1.

### Materials

In this investigation, Grade 4340 steel and mild steel were used. The chemical compositional ranges, and mechanical and physical properties for the materials used in this study are given in Tables 2–4, respectively.

The typical final shape of mild steel to mild steel bars and 4340 steel to mild steel bars obtained from the experiments is shown in Fig. 1A and B, respectively. Comprehensive information about the numerical and experimental phases of other materials can be found in Rahbar (Ref. 6).

### Modeling

In this investigation, the continuous friction welding process of Grade 4340 steel and mild steel was numerically simulated by the ABAQUS 6.4-11 Pro commercial software code (Ref. 7). The objective of the study was to consider the variations of temperature, deformation, stress, strain, and strain rate during the process. Moreover, in this study, the operational parameters of the friction welding process are related to the physical parameters of the process.

### Johnson-Cook Constitutive Equation

In the friction welding process, continuous rubbing of contact surfaces generates the heat at the weld interface. The temperature of the material increases with heat and therefore subsequent softening of the material occurs. The material at the interface starts to flow plastically and forms an upset collar. Therefore, the type of equation that can be used to describe the material behavior during the process must include the effect of temperature as well as strain and strain rate. Therefore, the Johnson-Cook equation (Ref. 8) is used in which the von Mises yield stress is defined as a function of strain, strain rate,

Table 1 — Friction Welding Parameters of the Various Experiments Performed

Materials	Initial Pressure (MPa)	Final Pressure (MPa)	Friction Time (s)	Rotation Speed (rev/min)
4340 Steel–4340 Steel	80	100	7	3000
Mild Steel–Mild Steel	20	30	6	3000
4340 Steel–Mild Steel	50	75	6	3000

Table 2 — Composition Ranges of the Materials Used in This Study

Grade		C	Mn	Si	P	S	Cr	Mo	Ni
4340 Steel	min.	0.38	0.6	0.15	—	—	0.7	0.2	1.65
	max.	0.43	0.8	0.30	0.035	0.04	0.9	0.3	2.0
Mild Steel	min.	0.03	0.2	—	—	—	—	—	—
	max.	1.25	16	0.5	0.05	0.05	—	—	—

Table 3 — Mechanical Properties of the Materials Used in This Study

Grade	Tensile Strength (MPa)	Yield Strength 0.2% Proof (MPa)	Elongation (% in 50 mm) min.	Rockwell C (HRC) max.
	min.	min.		
4340 Steel	744.6	473.2	22	39
Mild Steel	420	350	15	26

Table 4 — Physical Properties of the Materials Used in This Study

Grade	Density (kg/m <sup>3</sup> )	Elastic Modulus (GPa)	Mean Coefficient of Thermal Expansion (μm/m°C)			Thermal Conductivity (W/m.K)		Specific Heat 0°–100°C (J/kg.K)
			0°–100°C	0°–315°C	0°–538°C	at 100°C	at 500°C	
			4340 Steel	7700–8300	190–210	17.2	17.8	
Mild Steel	7800–8000	200	9.5–12.6	11.7	12.8	44		470

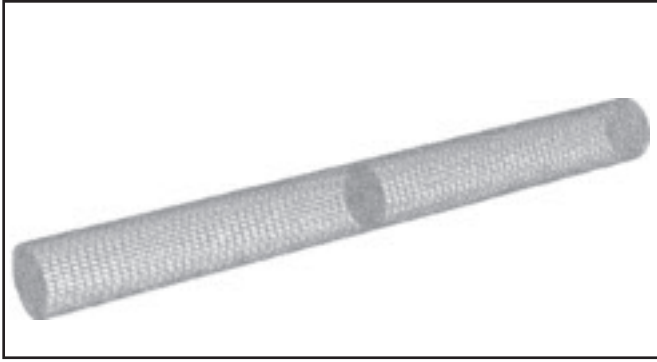


Fig. 2 — Initial configuration of the simulation of two bars before welding.

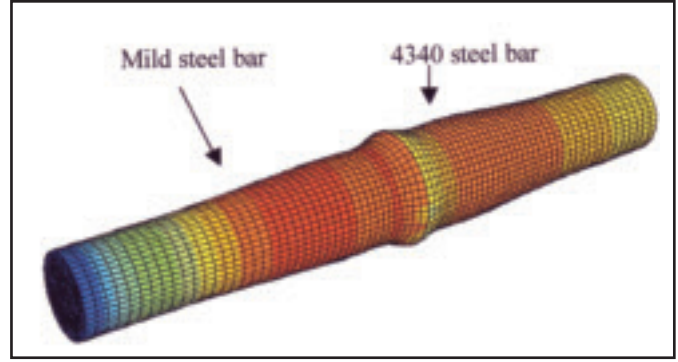


Fig. 3 — The final shape of the weld between stainless steel and mild steel.

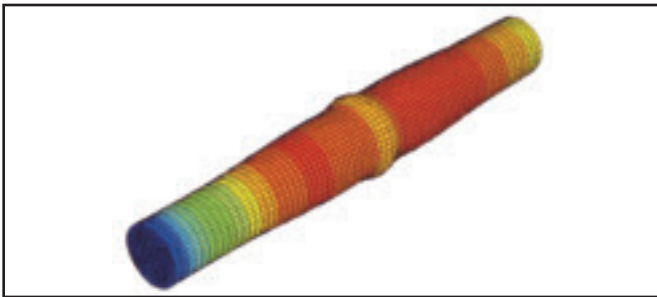


Fig. 4 — The final shape of the weld between mild steel and mild steel.

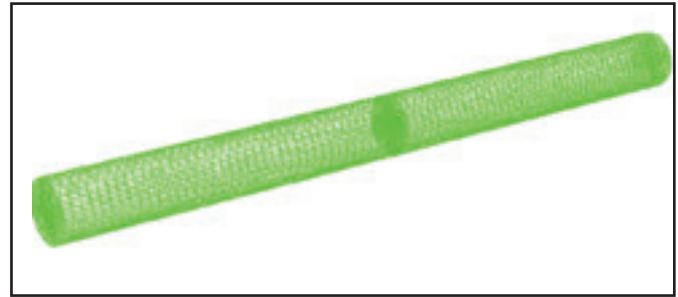


Fig. 5 — The "centerline" path upon which the analysis carried out in this paper is based.

and temperature, i.e.,

$$\sigma = \left( A + B\epsilon^n \right) \times \left( 1 + c \cdot \ln \dot{\epsilon}_p \right) \times \left( 1 - T^m \right) \quad (1)$$

where  $\epsilon$  is the equivalent plastic strain,  $\dot{\epsilon}_p$  is the plastic strain rate,  $T^\circ$  is the homologous temperature

$$\left( \frac{T - T_{room}}{T_{melt} - T_{room}} \right),$$

and  $T$  is the absolute temperature.  $A$ ,  $B$ ,  $n$ ,  $c$ , and  $m$  are five constants. The expression in the first set of brackets gives the stress as a function of strain for  $\dot{\epsilon}_p = 1$  and  $T^\circ = 0$ . The expressions in the second and third set represent the effects of strain rate and temperature, respectively. The Johnson-Cook parameters for the materials used in this study are tabulated in Table 5.

### The Finite Element Modeling of the Friction Welding Process

In this analysis, the eight-node element was used. The modeling was performed 3D with reduced integration points and

coupled temperature-displacement equations were employed. The C3D8RT element type was used. A proper contact algorithm was employed in the model. The general contact algorithm is used in modeling the friction welding process due to the following reasons:

- During the friction welding process, more than two surfaces can take part in contact.
- The edge of the materials must be included during the contact procedure.

In addition, an algorithm was written and coded into the software to express the contact definition of the process. Two-step modeling was used in order to suitably express the process. In the first step, rotating and transition speeds were applied to the left bar and when a certain amount of upsetting had occurred, the second step, the

rotation stopped and the compressive force was maintained or slightly increased to consolidate the weld. The boundary condition is defined so that the materials positioned in the right-hand side of the paper are fixed, and the materials suited in the left-hand side of the paper are rotating. According to this, the centerline nodes could only move in the "z" axis and not in "x" or "y" axis. The initial and final pressures are applied to the fixed bar. The initial pressure is applied during the welding time in which its values are increased to the final pressure during the braking time while the rotating speed decreases to zero. The adaptive mesh type was used to adjust with the grain refinement during the contact deformation process. Thermal effects are assumed to be adiabatic.

Table 5 — The Johnson-Cook Parameters for the Materials Used in This Study (Ref. 7)

Material	A (MPa)	B (MPa)	n	C	M
Mild Steel	310	350	0.3	0.02	0.5
4340 Steel	792	510	0.26	0.014	1.03

## Results of the ABAQUS Analyses and Experiments

Figure 2 shows the initial configuration of the process. The final configuration of the friction welding of 4340 steel bar to mild steel bar is shown in Fig. 3. The left-hand side of the model in Fig. 3 is the 4340 steel bar. The final shape of the mild steel bar to mild steel bar is depicted in Fig. 4. Comparing Figs. 1 and 3 shows that simulation is relatively successful in modeling the out shape of the weld. The thin edge of the upset produced in experimental results could not be achieved due to the limitation of element size and type and avoidance of more complexity.

### Validation of the Simulation Results

The sizes of upsetting occurring during the friction welding process were compared with the corresponding simulation results. The results are tabulated in Table 6. Validation of temperature results are described in the Hardness Distributions section of this paper.

To analyze the simulation results, a typical “centerline” path similar to what is shown in Fig. 5 is chosen. The path has 150 mm length and includes the weld zone, the heat-affected zones (HAZ), and parts of both base metals. The path starts at 50 mm from the left bar end to 50 mm from the right bar end. It covers all the changes that might occur during the friction welding process.

### Microstructures

The metallographic images of the mild steel to mild steel samples before and after welding are shown in Fig. 6A–C. Figure 6B, C shows the fine grain size structure produced at the HAZ and the weld zones, respectively. After cooling and applying the subsequent pressure, the process of recrystallization and growth takes place that results in a fine grain structure — Fig. 6C. The fusion zone has finer grain than the HAZ. Typical temperature profile obtained from the simulation is shown in Fig. 6D. Figure 6D shows a very high temperature is produced at the collision zone. In addition, it will be shown later in the section titled Plastic Strain Distributions that the very high plastic strain is produced at the collision zone. High-temperature and plastic strain with fast cooling results in a fine grain structure at the contact zone. According to the Hall-Petch equation, the material strength depends on the grain size, and smaller grains produce the higher strengths (strength test results are described in the next section).

Similar trends are seen in friction welding of other samples. Figure 7A, B shows

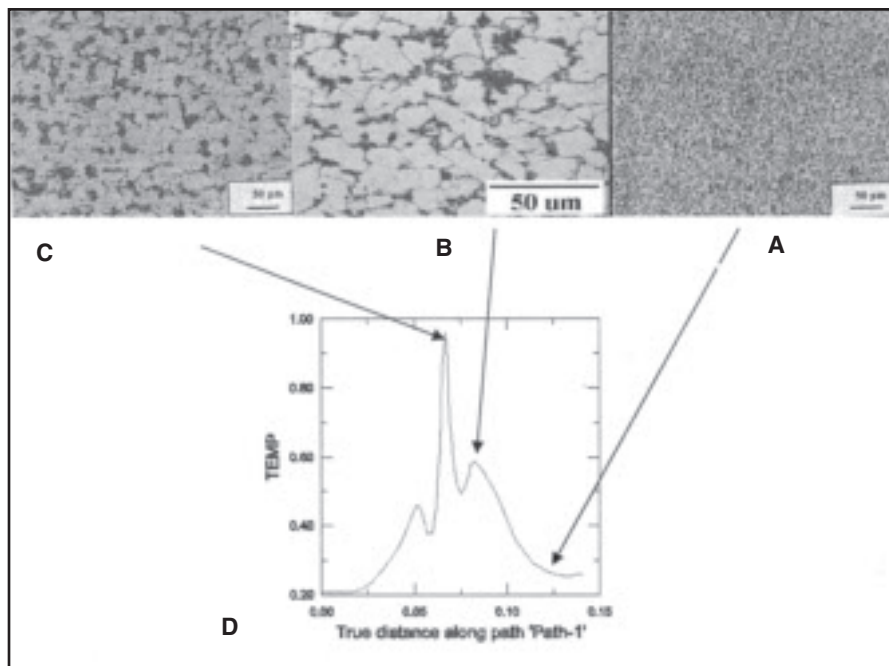


Fig. 6 — Metallographic images of the interface of a mild steel to mild steel friction weld: A — Initial mild steel structure before welding; B — the microstructure obtained after welding in the HAZ; C — the microstructure achieved in the fusion zone; D — temperature profile.

the metallographic images of the 4340 steel to mild steel samples before and after welding, respectively.

### The Tensile Tests

Experiments were also conducted to measure the weld strength of the samples. Figure 8A shows the tensile test of mild steel before the weld, and Fig. 8B depicts the tensile strength of the weld after the friction welding process. The two figures are similar showing the rupture occurs in the mild steel base bars and not at the weld zone.

### Hardness Distributions

The study was also conducted to find the hardness distributions across the joints. Figure 9 shows the typical hardness distributions (in Vickers) for the friction welded joints of 4340 steel-mild steel. Maximum hardness is obtained at the fu-

sion zones (which have a finer grain size). The hardness is decreased in the HAZ due to temperature softening and coarser grain size structure produced (see typical temperature profile in Fig. 6D and microstructure in Fig. 6B). In the experiments and the simulations, the bars were fixed at the right-hand side and rotating at the left-hand side of the figure. This produces some rigidity at the bar ends and causes the increase of hardness at a distance far away from the weld centerline. The increase in hardness away from the joints, which is due to fixing the bars during the test, is shown in Fig. 9.

### The Temperature Distributions

Friction causes the increase in temperature at the interface. The highest temperature is obtained at the weld centerline and the temperature decreases with distance away from the weld centerline. Figure 10A shows the temperature distribu-

Table 6 — Comparison of Upsetting Thickness between Simulations and Experiments

Materials	Size of Upsetting (Simulation) (mm)	Size of Upsetting (Experiments) (mm)	Comparison (% Error)
Mild Steel-Mild Steel	1.9	2	5
4340 Steel-4340 Steel	1.8	2	10
4340 Steel-mild Steel	2.3	2.2	4.5

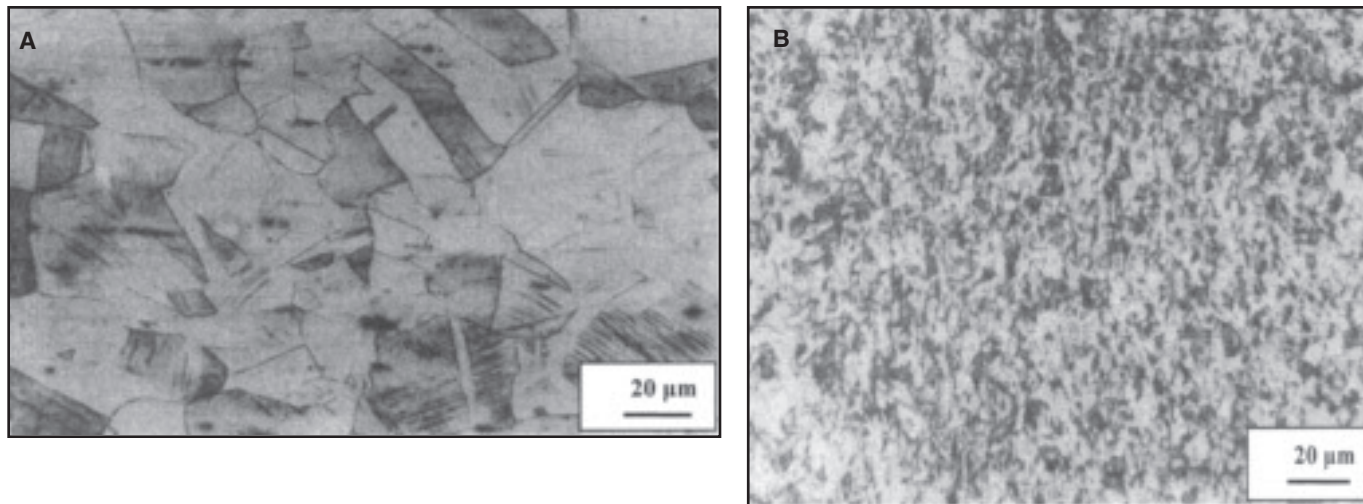


Fig. 7 — Metallographic images of the interface of 4340 steel to mild steel: A — The initial 4340 steel structure before welding; B — the microstructure achieved after welding in the fusion zone of 4340 steel-mild steel friction weld sample (initial mild steel structure is shown in Fig. 6A).

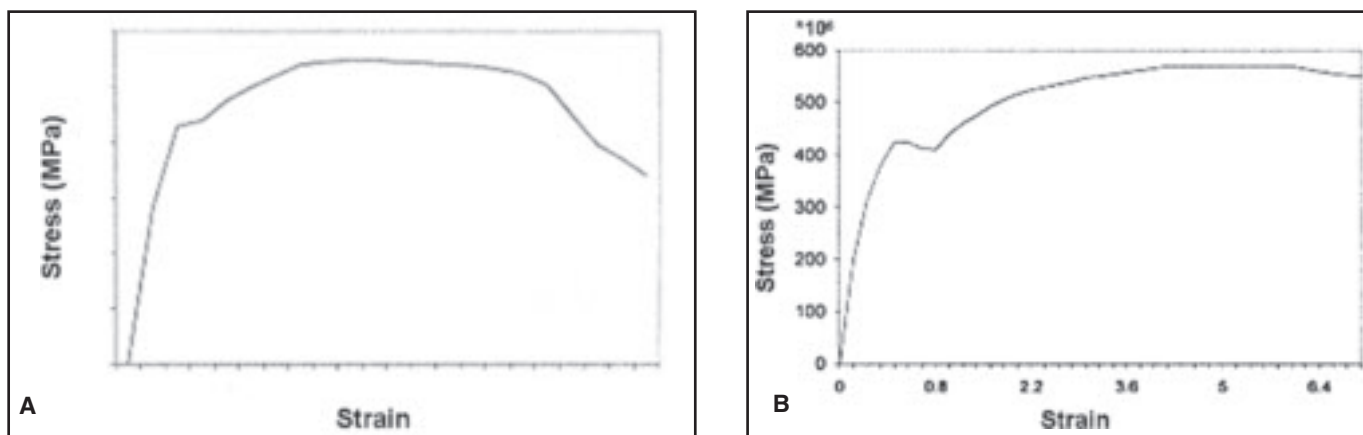


Fig. 8 — Stress-strain graphs: A — The mild steel specimen; B — the mild steel to mild steel weld.

tions for friction welding of 4340 steel to mild steel material bars, and Fig. 10B shows profiles for friction welding of mild steel to mild steel bars. The graphs are drawn based on the normalized temperature. The normalized temperature is the ratio of actual temperature to the melting point temperature in °C. The data on the figures show the ratio of actual temperature to the melting temperature for some critical points. The figures clearly show that the welding zones consist of two heat-affected zones and a center zone. Higher temperature is obtained for the friction welding of 4340 steel to mild steel materials. The heat-affected zone peak temperature is found to be lower in the right-hand sides of Fig. 10A and B than it is in the left-hand side of Fig. 10A and B. The difference is attributed to positioning the fixed bar to the right-hand side of the figures and suiting the rotating bar in the left-

hand sides of the figures and the initial and final pressures are applied to the fixed bars. The maximum temperatures measured by the infrared detector for the 430-mild steel and mild steel-mild steel combinations were 1425° and 1480°C, respectively. The corresponding simulation results predicted were 1440° and 1520°C, respectively.

### The Plastic Strain Distributions

The transient temperature produced in the friction zone causes the variations of all the physical parameters during the friction welding process. The plastic strain distributions are similar in shape to the temperature distributions. Figure 11A shows the plastic strain distributions for friction welding of 4340 steel to mild steel materials, and Fig. 11B depicts profiles for the friction welding of mild steel to mild

steel bars, respectively. The peak plastic strain is obtained at the centerline. The figures show that the plastic strain decreases with distance from the centerline. In the heat-affected zone, the plastic strain increases slightly due to the increase of temperature. The temperature decreases further at distances away from the heat-affected zones.

### The Von Mises Stress Distributions

Figure 12 shows the von Mises stress profiles for the two samples. In Fig. 12A, the von Mises stress profiles for friction welding of 4340 steel to mild steel are shown and in Fig. 12B, profiles for friction welding of mild steel to mild steel are depicted. The asymmetry in the von Mises stress profiles seen in Fig. 12A in comparison with Fig. 12B is attributed to welding dissimilar materials (i.e., 4340 steel to

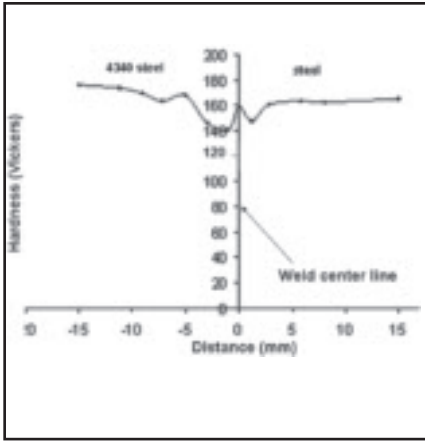


Fig. 9 — Typical hardness distributions of the 4340 steel-mild steel and A12017-A12017 samples.

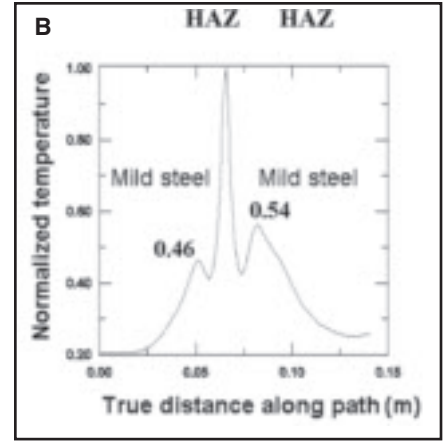
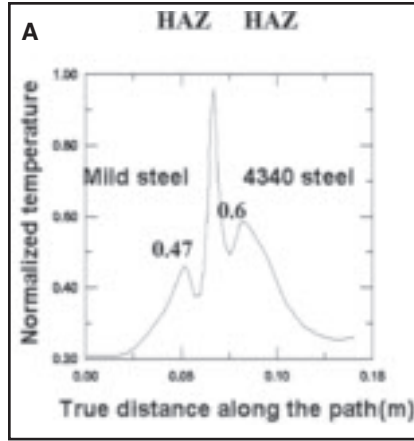


Fig. 10 — Normalized temperature profiles for friction welding of the following: A — 4340 steel to mild steel materials; B — mild steel to mild steel materials.

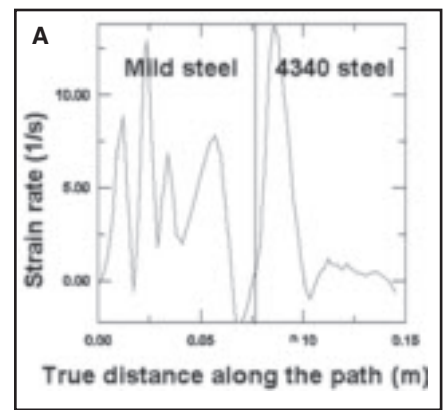
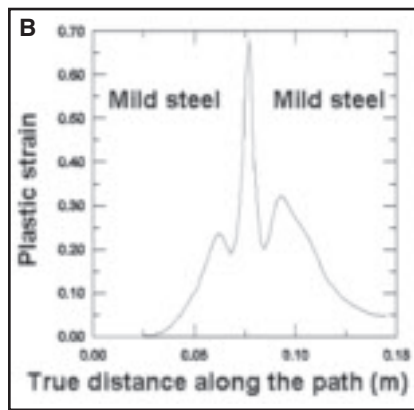
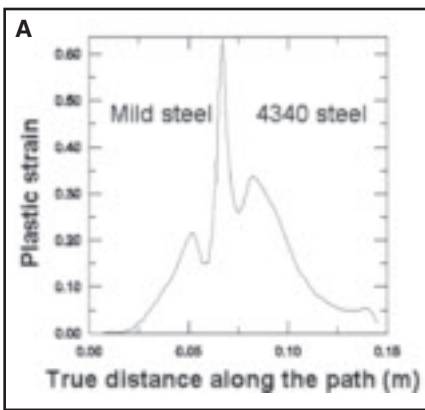


Fig. 11 — The plastic strain distributions for friction welding of the following: A — 4340 steel to mild steel materials; B — mild steel to mild steel materials.

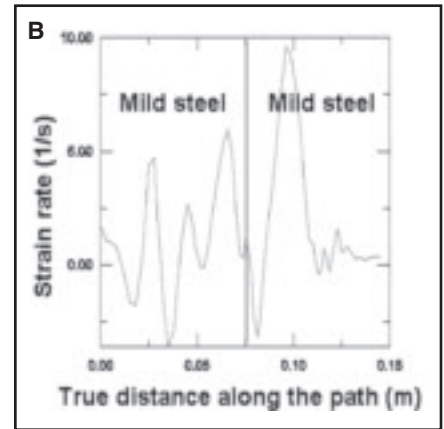
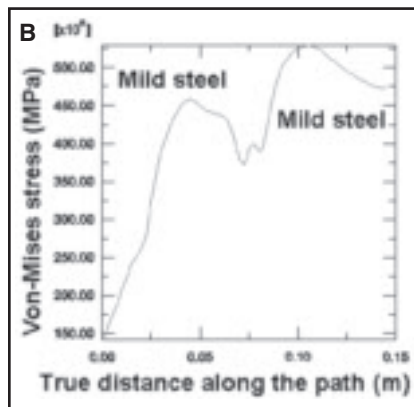
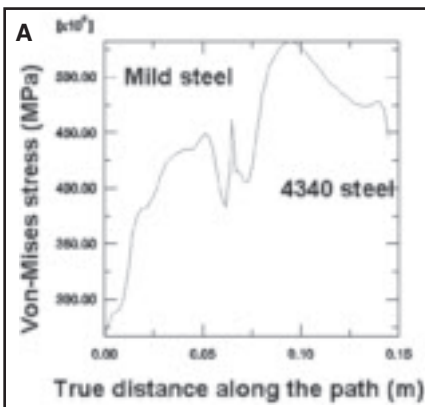


Fig. 12 — Von Mises stress distributions for friction welding of the following: A — 4340 steel to mild steel materials; B — mild steel to mild steel materials.

Fig. 13 — The strain rate distributions for friction welding of the following: A — 4340 steel to mild steel materials; B — mild steel to mild steel materials.

mild steel bars). In addition, the 4340 steel has more strength than the mild steel and therefore the von Mises stress in the right side of Fig. 12A is higher than that in the left side of the figure. In addition, a special pattern and characteristic exist in both figures and are described as follows: At a very far

distance from the weld centerline, the von Mises stress is found to be similar to the von Mises stress of material at room temperature, since the effects of temperature and deformation on the material are negligible. At a closer distance to the weld centerline, in the heat-affected zone, the temperature

increases and the yield stress at temperature decreases which, in turn, reduces the von Mises stress — Fig. 12A, B.

At a closer distance to the weld centerline, the increase of temperature produces more plasticity while the rest of the material resists against the deformation which, in

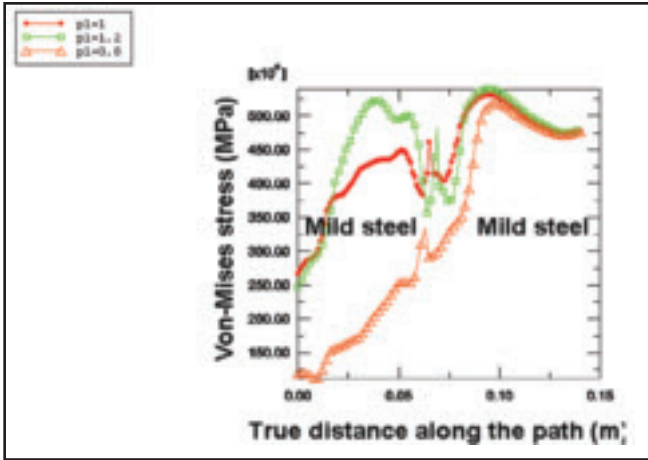


Fig. 14 — Effects of initial pressure on von Mises stress for constant final pressure on 4340 steel to mild steel.

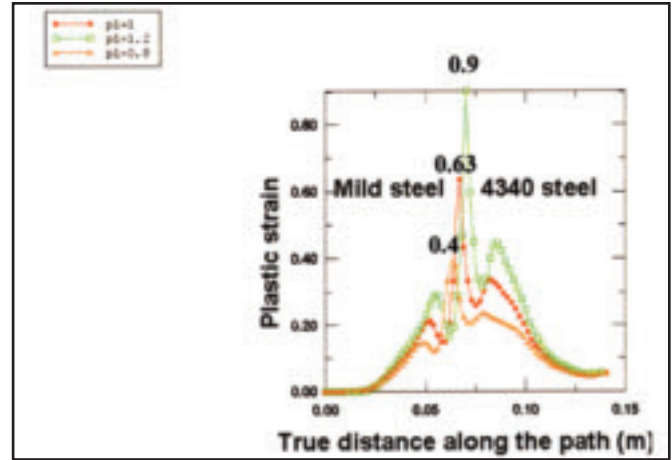


Fig. 15 — Effects of initial pressures on plastic strains for constant final pressure — 4340 steel to mild steel.

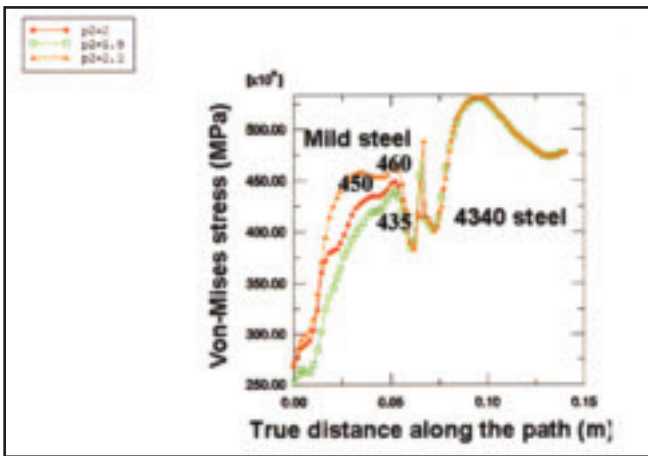


Fig. 16 — Effects of final pressures on von Mises stress for constant initial pressure — 4340 steel to mild steel.

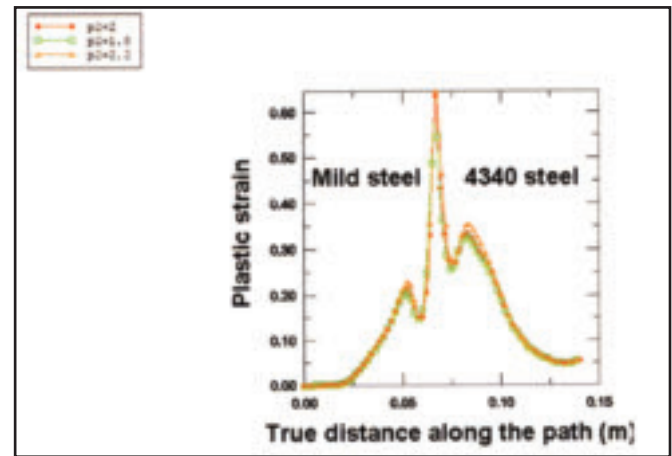


Fig. 17 — Effects of final pressures on equivalent strain profiles for constant initial pressure on 4340 steel to mild steel.

turn, increases the von Mises stress. At the weld centerline, where the two surfaces are in contact with each other, the von Mises stress reduces and the peak plastic strain increases due to temperature softening produced at the weld centerline. At distances away from the weld zones due to resistance of the material against the deformation, the von Mises stress increases. The von Mises stress obtained for the friction welding of 4340 steel to mild steel is found to be higher than that of mild steel to mild steel materials. This matter is attributed to friction welding of two dissimilar materials, which in turn produces more resistance to deformation due to the materials' yield stress variations at temperatures.

### The Strain Rate Distributions

The strain rate is an important physical parameter in plasticity. Therefore, the analysis was carried out to consider the strain rate distributions in the friction weld-

ing process. The most deformation occurred in the interface as a result of high transient temperature and subsequent material flowing. Figure 13A shows the strain rate distributions for friction welding of 4340 steel to mild steel materials, and Figure 13B illustrates the strain rate distributions for friction welding of mild steel to mild steel materials. Different strain rate patterns are obtained for friction welding of 4340 steel to mild steel and for mild steel to mild steel materials, respectively. In general, the strain rate of the order of  $10^1$  observed for friction welding of 4340 steel to mild steel materials compared to the strain rate of the order 1 obtained for friction welding of mild steel to mild steel materials. Strain rate variations for the mild steel to mild steel friction weld are wider than those for the 4340 steel to mild steel friction weld. However, the figures show that the strain rate is zero at the weld interface due to temperature softening and might be positive and negative in the heat-affected zone, de-

creasing from zero to a minimum value and reaching again at  $x = 0$ ; to rise to a maximum positive at the heat-affected zone. This variation of the strain rate is seen in modeling of all samples. The strain rate approaches zero at a far distance since no deformation occurred at distances away from the weld and HAZ zones. More fluctuation of the strain rate was observed in the material's left-hand side than in the right-hand side. The reason is attributed to fixing of the right-hand-side bar and rotation of the left-hand-side bar. The strain rate fluctuations are increased with the bar rotation velocity.

### Effects of Initial Pressure on Internal Parameters

#### Effects of Initial Pressure on Von Mises Stress

Figure 14 shows the effects of initial pressure on the von Mises distributions for friction welding of mild steel to mild

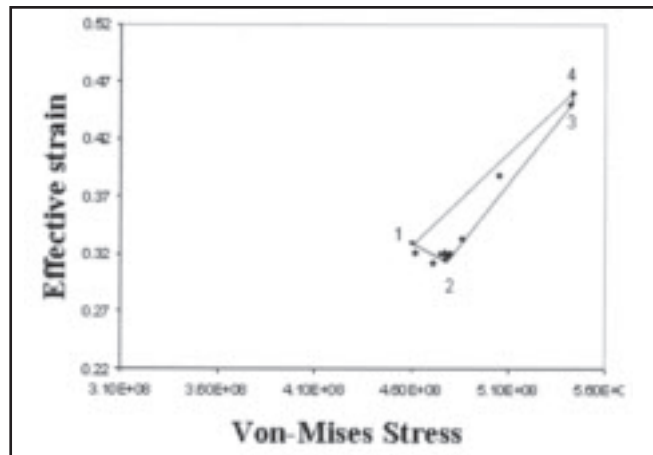
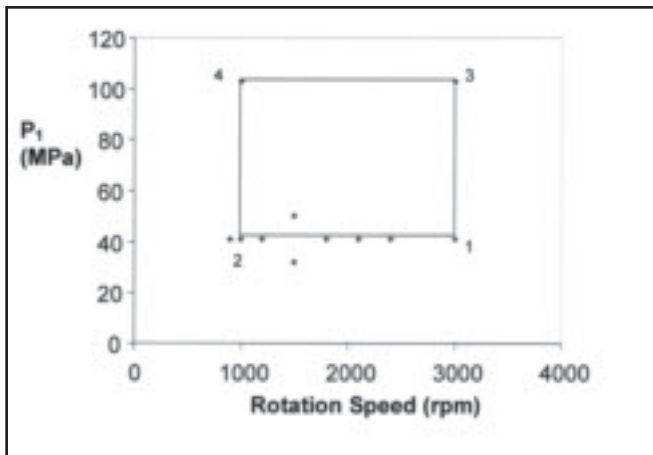


Fig. 18 — The experimental welding window.

Fig. 19 — The numerical welding window.

steel bars when the final pressure is kept constant. Three initial pressures were chosen — 0.8 (in yellow), 1.2 (in green), and 1 (in red) — times the initial pressure from Table 1. The numbers in the figures show the magnitude of von Mises stresses for that point. The simulation results show that all the diagrams follow similar patterns. Simulation results show that the von Mises stress increases with the initial pressure. Increase of pressure to the ratio of 1.2 causes the von Mises stress to increase about 50 MPa. The figure shows that the initial pressure does not affect the von Mises stress for the fixed bar (see the right-hand sides of the profiles in Fig. 14). Moreover, the magnitude of von Mises stress at the contact surface (fusion zone) increases with initial pressure. This matter is attributed to more hardening occurring in the fusion zones by increasing the initial pressure. In addition, Fig. 14 shows that the initial pressure of 16 MPa (0.8 P) is not sufficient to produce deformation and plasticity. It is also implied that the initial pressure is an important parameter that helps with plasticity similar to rotational velocity.

#### Effects of Initial Pressure on Plastic Strain

Figure 15 shows the effects of initial pressure on the plastic strain profiles for friction welding of mild steel to 4340 steel bars when the final pressure is kept constant. The highest plastic strains occurred at the contact zones. Simulation results show that the plastic strain at the contact zone increases with the initial pressure. The numbers in the figure show the magnitude of plastic strain at the fusion zones. In addition, the figure shows that the fusion zones shift toward the fixed bar (to the right-hand side) by increasing the ini-

tial pressure, which in turn causes an increase in pressure and plasticity at the contact surface.

#### **Effects of Final Pressure on Internal Parameters**

##### Effects of Final Pressure on Von Mises Stress

Figure 16 shows the effects of final pressure on the von Mises stress distributions for friction welding of mild steel to 4340 steel bars when the initial pressure is kept constant. Three final pressure ratios of 1.8, 2, and 2.2, to the defined final pressure in Table 1, were selected for simulations. Figure 16 also shows the von Mises stress along the rods.

Simulation results show that the final pressure does not significantly affect the von Mises stress obtained at the fusion zone and on the fixed bar. However, the von Mises stress increases slightly in the rotating bar with the final pressure. In other words, the HAZ von Mises stress increases in the rotating bar with the final pressure. Comparison between Figs. 14 and 16 reveals that initial pressure is a more important parameter than final pressure in affecting the von Mises stress.

##### Effects of Final Pressure on Equivalent Strain

Figure 17 shows the effects of final pressure on the equivalent strain distributions for friction welding of mild steel to 4340 steel bars when the initial pressure is kept constant.

The simulation results show that the effective strain distributions are not affected by the final pressure. Comparison between Figs. 14 and 17 reveals that initial pressure is more effective than final pres-

sure on changing the effective strain profiles.

#### **The Proposed Experimental and Physical Welding Windows**

It is possible to draw a welding window based on the experimental parameters. The two most important experimental parameters are the rotational velocity and the initial pressure. It was found previously that the initial pressure is more important than the final pressure. Figure 18 shows the welding window for the 4340-mild steel combinations. In any welding window, minimum values of pressure and rotational velocity are required in order to produce the weld. If the initial pressure and rotational velocity are below these limits, there would not be enough plastic deformation to consolidate the weld. Moreover, there exists maximum pressure and rotational velocity. If the initial pressure exceeds a threshold limit, it may result in cracking and distortion of the materials. If the rotational velocity exceeds a threshold limit, it produces more heat at the temperature and more softening and may produce melt at the interface and, therefore, there would be no weld in the interface.

It is also possible to draw the numerical welding window based on the numerical parameters. It was found from this study that the most influential numerical parameters are the von Mises stress and the effective strain. Figure 19 shows the numerical welding window for the 4340-mild steel combinations. In the numerical welding window, it is not possible to draw a line of minimum and maximum von Mises and effective strain similar to what can be drawn for the initial pressure and rotational velocity welding window. This

may be attributed to more dependency on variables such as the von Mises and effective strain to those of initial pressure and rotational velocity. The numerical welding window shows the welding window boundaries. As long as the numerical values of von Mises and effective strain obtained from any operational parameters used are inside the window, we can suggest that welding may occur.

The numerical welding window makes it possible to find the required essential operational parameters for friction welding of any combinations. This proposal may help in reducing lots of trial and error experiments carried out to produce the weld for any similar and dissimilar combinations.

## Conclusions

Numerical calculations and experiments were performed to analyze the continuous friction welding process, which is a typical process with a high temperature, large deformation, and transient operation. The mathematical model of continuous friction welding is presented. The coupled effects of the mechanics and heat transfer are taken into account in the model. The distributions of temperature, deformation, von Mises stress, strain, and strain rate during the continuous friction welding process were numerically analyzed. The simulation results of temperature were in good agreement with the experimental points. The shape of the upset collar obtained from the simulations also fits excellently with those experimentally observed. With the finite element method (FEM) used in this paper, distribution of welding temperature, flow stress, and plastic strain and strain rate can be ob-

tained. That means this model can be used as an industrial tool to predict evolution of temperature, stress, strain, and final geometry of the welded parts.

The following conclusions can be drawn from this study.

- Simulation results predict a high value of plastic strain produced at the weld centerline due to increasing the temperature.
- Similar trends to those obtained with the plastic strain distributions are obtained for the temperature distributions.
- The peak von Mises stress is produced at distances away from the weld centerlines.
- The von Mises stress reduces in the fusion zone due to temperature softening.
- The von Mises stress obtained for friction welding of 4340 steel to mild steel is found to be higher than that achieved for friction welding of mild steel to mild steel materials. This is attributed to friction welding of two dissimilar materials, which in turn produces more resistance to deformation, and is also due to the materials yield stress variations at temperatures.
- A very fine grain structure is produced at the weld zone, which in turn causes the higher strength according to the Hall-Petch relation.
- The results of the tensile test predict that the weld zone is stronger than the base metals since the rupture occurred outside of the welding area.
- The shape of the upsetting obtained from the simulation is similar to that achieved from the experiments.
- The initial pressure is a more effective parameter than the final pressure on changing the von Mises stress and

equivalent strain distributions.

- The experimental and numerical welding windows are proposed to determine the operational and numerical parameters to produce the weld.

## References

1. Vairis, A., and Frost, M. 2000. Modeling the linear friction welding of titanium blocks. *Journal of Material Science and Engineering A292*: 8–17.
2. Sluzalec, A. 1988. Thermal effects in friction welding. *International Journal of Mechanical Science* 32(6): 467–478.
3. Fu, L., and Duan, L. 1988. The coupled deformation and heat flow analysis by finite element method during friction welding. *Welding Journal* 77(5): 202-s to 207-s.
4. Alvise, L. D., and Massoni, E. 2002. Finite element modeling of the inertia friction welding process between dissimilar materials. *Journal of Materials Processing Technology*, 125-126: 387–391.
5. Sahin, M. 2004. Simulation of friction welding using a developed computer program. *Journal of Materials Processing Technology*. 153-154: 1011–1018.
6. Rahbar Kelishami, A. 2005. Thermomechanical analysis of friction welding by finite element method and its metallurgical relations, MSc thesis, Tehran, Iran, University of Tehran.
7. ABAQUS 6.4 Pro11 software, Help, 2005.
8. Johnson, R. G., and Cook, W. H. 2004. A constitutive model and data for metals subjected to large strains, high strain-rates and high temperature. *Proc. of the 7th Int. Symp. BALESTICS*, The Hague, The Netherlands, pp. 541–547.

## Call for Papers

### 2008 World Standards Day Competition

Sponsored by the Standards Engineering Society (SES), the theme for this year's paper competition, "Intelligent and Sustainable Buildings," recognizes the critical role of standards and conformity assessment programs in ensuring safety requirements; facilitating coordination among contractors, builders, engineers, and architects; and incorporating new technologies in design and construction. The competition invites papers that use specific examples to show ways that standards and conformity assessment programs are used for intelligent and sustainable buildings.

All paper contest submissions must be received with an official entry form by midnight on August 29, 2008, by the SES Executive Director, 13340 SW 96th Avenue, Miami, Florida, 33176. For details on the winners' recognition, cash awards, judging, and rules, go to [www.ses-standards.org](http://www.ses-standards.org) and follow the link for WSD Paper Competition 2008.